

Electronic Supplementary Information

A Metal-Organic Framework as a Flask: Photophysics of Confined Chromophores with a Benzylidene Imidazolinone Core

E. A. Dolgoplova, T. M. Moore, O. A. Ejegbavwo, P. J. Pellechia, M. D. Smith, and
N. B. Shustova*

*Department of Chemistry and Biochemistry, University of South Carolina, Columbia, 29208,
United States*

Table of contents:	page number
1. Materials	S2
2. Synthesis of <i>p</i> COOH-BI	S2
3. Synthesis of <i>p</i> COOH-BI-CO ₂ Me	S3
4. Synthesis of MeO- <i>o</i> HBI@MOF	S3
5. Peptide coupling procedure	S3
6. X-ray crystal structure determination	S3
7. Fluorescence spectroscopy	S5
8. ² H NMR spectroscopy	S5
9. Other physical measurements	S5
10. Table S1. X-ray structure refinement data for <i>p</i> COOH-BI-CO ₂ Me and <i>p</i> COOH-BI	S6
11. Figure S1. PXRD patterns of MeO- <i>o</i> HBI@MOF materials	S7
12. Figure S2. Crystal structure of <i>p</i> COOH-BI	S8
13. Figure S3. ¹ H and ¹³ C NMR spectra of <i>p</i> COOH-BI	S9
14. Figure S4. FT-IR spectrum of <i>p</i> COOH-BI	S10
15. Figure S5. Crystal structure of <i>p</i> COOH-BI-CO ₂ Me	S11
16. Figure S6. ¹ H and ¹³ C NMR spectra of <i>p</i> COOH-BI-CO ₂ Me	S12
17. Figure S7. FT-IR spectrum of <i>p</i> COOH-BI-CO ₂ Me	S13
18. Figure S8. Normalized emission spectra of <i>p</i> COOH-BI-CO ₂ Me and <i>p</i> COOH-BI	S14
19. Figure S9. PXRD patterns of Zr ₆ O ₄ (OH) ₄ (BDC-BI- <i>d</i> ₃) ₆	S15
20. Figure S10. Solid state ² H NMR of Zr ₆ O ₄ (OH) ₄ (BDC-BI- <i>d</i> ₃) ₆	S15
21. Figure S11. ¹ H NMR spectrum of digested UiO-68-NH ₂ coupled with <i>p</i> COOH-BI	S16
22. Figure S12. ¹ H NMR spectrum of digested UiO-68-NH ₂ coupled with <i>p</i> COOH-BI-CO ₂ Me	S16
23. Figure S13. ¹ H NMR spectrum of digested MIL-101-Al-NH ₂ coupled with <i>p</i> COOH-BI	S17
24. Figure S14. ¹ H NMR spectrum of digested UiO-68-NH ₂ coupled with <i>p</i> COOH-BI-CO ₂ Me	S17
25. References	S18

Materials.

Zn(NO₃)₂·6H₂O (technical grade, Ward's Science), ZrCl₄ (99.5%, Alfa Aesar), Zr(NO₃)₄·5H₂O (99.99%, Energy Chemical), AlCl₃·6H₂O (99%, Alfa Aesar), CsF (99%, Oakwood Chemical), KOH (ACS grade, Fisher Chemical), K₂CO₃ (ACS grade, BDH), 1,3,5-benzenetricarboxylic acid (98%, Alfa Aesar), terephthalic acid (>99%, TCI America), 2-aminoterephthalic acid (>98%, TCI America), 4,4'-biphenyldicarboxylic acid (97%, Oakwood Chemical), 1,3,5-tribromobenzene (> 95%, Matrix Scientific), 4-methoxycarbonyl phenylboronic acid (>97%, Boronic Molecular), 4-carboxyphenylboronic acid (99.5%, Chem-Impex International Inc.), 2,5-dibromoaniline (97%, Oakwood Chemical), palladium(II) acetate (> 95%, Ox-Chem), triphenylphosphine (99%, Sigma-Aldrich), polyethylene glycol 400 (lab grade, Merck Millipore), 2-hydroxy-5-methoxy-benzaldehyde (95%, Oxchem), 4-carboxybenzaldehyde (99%, Chem-Impex International Inc.), *N,N'*-diisopropylcarbodiimide (DIC, >99%, Oakwood Chemical), glycine methyl ester hydrochloride (98%, Acros Organics), ethyl acetimidate hydrochloride (97%, Alfa Aesar), methyl-amine (33% solution in absolute ethanol, Sigma Aldrich), 4-bromo-3-methyl benzoic acid methyl ester (99.1%, Chem-Impex International Inc.), chromium(VI) oxide (99.9%, Sigma-Aldrich), trans-dichlorobis(triphenylphosphine)palladium(II) (99%, Strem Chemicals), sodium hydroxide (ACS grade, Macron Fine Chemicals), acetic anhydride (99.6%, Chem-Impex International Inc.), sulfuric acid (ACS grade, Fischer Scientific), hydrochloric acid (ACS grade, Fischer Scientific), glacial acetic acid (ACS grade, BDH), trifluoroacetic acid (99%, Sigma Aldrich), diethyl ether (ACS grade, J. T. Baker® Chemicals), *N,N'*-dimethylformamide (ACS grade, BDH), hexane (ACS grade, Macron Fine Chemicals), tetrahydrofuran (ACS grade, Macron Fine Chemicals), ethanol (ACS grade, Decon Laboratories, Inc.), methanol (ACS grade, Fischer Scientific), acetonitrile (ACS grade, Fischer Scientific), DMSO-*d*₆ (Cambridge Isotope Laboratories, Inc.), sodium deuterioxide (40% w/w solution in D₂O, Alfa Aesar) and methanol-*d*₄ (Cambridge Isotope Laboratories, Inc.) were used as received.

The compounds methyl-2-((1-ethoxyethylidene)amino)acetate,¹ 5-(2-hydroxy-5-methoxybenzylidene)-2,3-dimethyl-3,5-dihydro-4*H*-imidazol-4-one (MeO-*o*HBI),² MIL-101-Al-NH₂,³ Zn₃(BTC)₂ (BTC = benzene-1,3,5-tricarboxylate),⁴ MOF-5,⁵ UiO-66 (UiO = University of Oslo),⁶ UiO-67,⁶ UiO-68-NH₂,⁶ Zn₃(BTB)₂ (BTB = benzene-1,3,5-tribenzoate),⁷ Zn₆(BTB)₄(BP)₂ (BP = 4,4'-bipyridyl),⁸ Zr₆O₄(OH)₄(BTB)₂,⁹ and Zr₆O₄(OH)₄(BDC-BI)₆ (BDC-BI = 2-((1-(2-methoxy-2-oxoethyl)-2-methyl-5-oxo-1,5-dihydro-4*H*-imidazol-4-ylidene)methyl)-[1,1'-biphenyl]-4,4'-dicarboxylate)² were prepared according to the reported procedures.

4-((1,2-dimethyl-5-oxo-1,5-dihydro-4*H*-imidazol-4-ylidene)methyl)benzoic acid (C₁₃H₁₂N₂O₃, *p*COOH-BI). The compound was prepared through adaptation of a literature procedure.¹ A methylamine solution (33% in ethanol, 3.78 g, 40.2 mmol) was added to 4-carboxybenzaldehyde (0.500 g, 3.30 mmol), and the resulting solution was stirred for 24 h at room temperature. Methyl-2-((1-ethoxyethylidene)amino)acetate (0.830 g, 5.22 mmol) and a catalytic amount of acetic acid (40.0 mg, 0.700 mmol) were added after 16 h, and the resulted mixture was stirred vigorously for an additional 6 h at room temperature. The precipitate was collected by filtration, washed with water and diethyl ether and dried under vacuum overnight. After drying under vacuum, *p*COOH-BI was isolated in 68% yield. ¹H NMR (DMSO-*d*₆, 300 MHz): δ = 2.37 (3H, s), 2.38 (3H, s), 6.96 (1H, s), 7.87 (2H, d, *J* = 7.91 Hz), 8.13 (2H, d, *J* = 8.32 Hz) (Figure S3). ¹³C NMR (DMSO-*d*₆, 400 MHz): δ = 15.87, 24.88, 26.75, 124.95, 129.57,

131.59, 135.20, 139.43, 165.06, 169.42, 170.36 (Figure S3). IR (neat, cm^{-1}): 2998, 1704, 1649, 1580, 1532, 1424, 1366, 1289, 1180, 1131, 987, 931, 908, 865, 853, 814, 787, 763, 704 (Figure S4). HRMS (ESI, m/z) calculated for $\text{C}_{14}\text{H}_{12}\text{N}_2\text{O}_5$ $[\text{M}+\text{H}]^+$ 245.0921, found 245.0919. Single crystal X-ray data for *p*COOH-BI are shown in Table S1 and Figure S2.

4-((1-(carboxymethyl)-2-methyl-5-oxo-1,5-dihydro-4H-imidazol-4-ylidene)methyl)benzoic acid ($\text{C}_{14}\text{H}_{12}\text{N}_2\text{O}_5$, *p*COOH-BI- CO_2Me). The prepared methyl-2-((1-ethoxyethylidene)amino)acetate (1.59 g, 9.99 mmol) was added to a solution of 4-carboxybenzaldehyde (0.500 g, 3.30 mmol) in 7.5 mL EtOH. After the resulted mixture was refluxed for 4 h, the yellow precipitate was collected through filtration and washed with ethanol, water and hexane. After drying under vacuum, *p*COOH-BI- CO_2Me was isolated in 65% yield. ^1H NMR ($\text{DMSO}-d_6$, 300 MHz): δ = 2.34 (1H, s), 3.71 (3H, s), 4.24 (s, 2H), 7.08 (1H, s), 7.98 (d, 2H, J = 7.96 Hz), 8.30 (d, 2H, J = 8.01 Hz), 13.2 (s, 1H) (Figure S6). ^{13}C NMR ($\text{DMSO}-d_6$, 400 MHz): δ = 15.75, 41.72, 53.03, 124.61, 129.93, 131.90, 132.34, 138.37, 140.03, 165.18, 167.36, 168.97, 169.81 (Figure S6). IR (neat, cm^{-1}): 2548, 1683, 1650, 1554, 1412, 1366, 1319, 1291, 1211, 1148, 986, 907, 865, 801, 778, 699 (Figure S7). HRMS (ESI, m/z) calculated for $\text{C}_{14}\text{H}_{12}\text{N}_2\text{O}_5$ $[\text{M}+\text{H}]^+$ 303.0975, found 303.0973. Single crystal X-ray data for *p*COOH-BI- CO_2Me is shown in Table S1 and Figure S5.

Synthesis of MeO-*o*HBI@MOF. Incorporation of MeO-*o*HBI inside MOFs was performed during solvothermal synthesis of corresponding framework. Solutions for preparation of MOFs (MOF-5,⁵ UiO-67,⁶ UiO-66,⁶ $\text{Zn}_3(\text{BTB})_2$,⁷ $\text{Zn}_6(\text{BTB})_4(\text{BP})_2$,⁸ $\text{Zr}_6\text{O}_4(\text{OH})_4(\text{BTB})_2$,⁹ UiO-68- NH_2 ⁶) were made according to reported literature procedures, in which 50 mg of MeO-*o*HBI was added. The resulted solutions underwent solvothermal treatment reported for MOF formation. The obtained crystals were thoroughly washed with DMF to remove residual chromophore molecules on MOF surface. To extract the chromophore from the pores the MeO-*o*HBI@MOF samples were sonicated and soaked in DMF for more than 6 hours. The amount of chromophore inclusion was quantified using calibration curves obtained from solutions with known concentrations by UV-vis spectroscopy. Loadings of the chromophores after incorporation for MOF-5, UiO-67, UiO-66, $\text{Zn}_3(\text{BTB})_2$, $\text{Zn}_6(\text{BTB})_4(\text{BP})_2$, $\text{Zr}_6\text{O}_4(\text{OH})_4(\text{BTB})_2$, and UiO-68- NH_2 were found to be 0.31, 0.47, 0.37, 0.30, 0.48, 0.070, and 0.17 wt%, respectively. The PXRD patterns of the prepared MeO-*o*HBI@MOF materials are shown in Figure S1.

Peptide coupling procedure. After 35 mg of UiO-68- NH_2 or MIL-101-Al- NH_2 was soaked in 3 mL of acetonitrile for 10 min, 200 μL of *N,N'*-diisopropylcarbodiimide and 50 mg of corresponding chromophores were added. After the resulted mixture was heated at 100 $^\circ\text{C}$ for 24h in a pressure flask, the solid material was isolated by filtration and washed three times with DMF.

Digestion procedure. To study the composition of the obtained materials by ^1H NMR spectroscopy, a solution of 450 μL of methanol- d_4 and 10 μL of sodium deuterioxide was added to 5 mg of the resulted solid, followed by sonication until complete sample dissolution. The ^1H NMR spectra of digested samples are shown in Figures S11-S14.

X-ray crystal structure determination.

***p*COOH-BI- CO_2Me** ($\text{C}_{14}\text{H}_{12}\text{N}_2\text{O}_5$). X-ray intensity data from a colorless almond-shaped plate were collected at 100(2) K using a Bruker D8 QUEST diffractometer equipped with a PHOTON

100 CMOS area detector and an Incoatec microfocus source (Mo K α radiation, $\lambda = 0.71073$ Å).¹⁰ The raw area detector data frames were reduced and corrected for absorption effects using the SAINT+ and SADABS programs.¹⁰ Final unit cell parameters were determined by least-squares refinement of 7317 reflections taken from the data set. The structure was solved by direct methods with SHELXT.^{11,12} Subsequent difference Fourier calculations and full-matrix least-squares refinement against F^2 were performed with SHELXL-2014^{11,12} using OLEX2.¹³

The compound crystallizes in the triclinic system. The space group $P-1$ was assumed and confirmed by structure solution. The asymmetric unit consists of two crystallographically independent but chemically similar molecules. The molecules were numbered identically except for label suffixes A or B. All non-hydrogen atoms were refined with anisotropic displacement parameters. Hydrogen atoms bonded to carbon were located in Fourier difference maps before being placed in geometrically idealized positions and included as riding atoms with $d(\text{C-H}) = 0.95$ Å for =CH hydrogen atoms, $d(\text{C-H}) = 0.99$ Å for methylene hydrogen atoms, and $d(\text{C-H}) = 0.98$ Å for methyl hydrogen atoms. The methyl hydrogen atoms were allowed to rotate as a rigid group to the orientation of maximum observed electron density. Isotropic displacement parameters for these H atoms were allowed to refine freely. The carboxylic group hydrogen atoms were located in difference maps. H3A, H3B, and H5B (bonded to O3A, O3B and O5B, respectively) were refined freely. Two electron density peaks corresponding to hydrogen atoms were observed near both O4A and O5A, suggesting two-fold disorder of this carboxylic acid group. This correlates with the nearly equivalent C14A–O4A and C14A–O5A bond distances (1.26 and 1.28 Å). Hydrogen atoms H4A and H5A were refined with half-occupancy with a common isotropic displacement parameter. The largest residual electron density peak in the final difference map is $0.90 \text{ e}^-/\text{\AA}^3$, located 0.98 Å from N2B. This and the other largest difference map features suggest minor whole-molecule disorder of molecule “B”. This disorder could not be successfully modeled because of its small population fraction, estimated at $< 5\%$ from trial modeling attempts.

***p*COOH-BI** ((C₁₃H₁₁N₂O₃H)(C₁₃H₁₁N₂O₃)(H₂O)_{1.12}(CH₃OH)_{0.83}). X-ray intensity data from a yellow rectangular bar crystal were collected at 100(2) K using a Bruker D8 QUEST diffractometer equipped with a PHOTON-100 CMOS area detector and an Incoatec microfocus source (Mo K α radiation, $\lambda = 0.71073$ Å). The raw area detector data frames were reduced and corrected for absorption effects using the Bruker APEX3, SAINT+ and SADABS programs.^{10,14} Final unit cell parameters were determined by least-squares refinement of 9725 reflections taken from the data set. The structure was solved with SHELXT.^{11,12} Subsequent difference Fourier calculations and full-matrix least-squares refinement against F^2 were performed with SHELXL-2016^{11,12} using OLEX2.¹³

The compound crystallizes in the triclinic system. The space group $P-1$ (No. 2) was confirmed by structure solution. The asymmetric unit consists of two crystallographically independent C₁₃H₁₁N₂O₃ molecules and a region of disordered electron density modeled as water and methanol. The two C₁₃H₁₁N₂O₃ molecules were numbered identically except for atom label suffixes A or B. Both are located near crystallographic inversion centers, with carboxylate oxygens O2B and O3A of each molecule close to a center. Carboxylic hydrogen atom positions could be located for O2B and O3A. They are disordered across the inversion center and were refined with half-occupancy, producing reasonable H2B and H3A displacement parameters. This generates an average of one neutral (protonated) carboxylic and one anionic carboxylate species per formula unit, and requires a charge-balancing cationic species elsewhere in the crystal. The

disordered solvent species were modeled with three water oxygen atoms and one methanol molecule. All solvent species refined to partial occupancy. The occupancies of methanol O1S/C1S and water O2S refined to 0.826(4) and 0.834(6), respectively, and water oxygens O3S and O4S to 0.172(4) and 0.116(5), respectively. The charge-compensating proton necessary for crystal electroneutrality is likely located among these species, but could not be reliably located because of the disorder and was not calculated. It is likely distributed across multiple atoms. The methanolic proton H1S and two hydrogen atoms for major water of H_3O^+ disorder component O2S could be located and refined isotropically with $d(\text{O-H}) = 0.85(2)$ Å distance restraints. All non-hydrogen atoms were refined with anisotropic displacement parameters except for minor water oxygens O3S and O4S, which were refined with a common isotropic displacement parameter. Hydrogen atoms bonded to carbon were located in Fourier difference maps before being placed in geometrically idealized positions and included as riding atoms with $d(\text{C-H}) = 0.95$ Å and $U_{\text{iso}}(\text{H}) = 1.2U_{\text{eq}}(\text{C})$ for aromatic hydrogen atoms and $d(\text{C-H}) = 0.98$ Å and $U_{\text{iso}}(\text{H}) = 1.5U_{\text{eq}}(\text{C})$ for methyl hydrogens. The methyl hydrogen atoms were allowed to rotate as a rigid group to the orientation of maximum observed electron density. The largest residual electron density peak in the final difference map is $0.45 \text{ e}^-/\text{\AA}^3$, located 1.05 Å from O1S.

Fluorescence spectroscopy.

Steady-state emission spectra were acquired on an Edinburgh FS5 fluorescence spectrometer equipped with a 150 W Continuous Wave Xenon Lamp source for excitation. Emission measurements on solid samples were collected on powders of the appropriate materials and placed inside a 0.5 mm quartz sample holder using the front-facing module. An Ocean Optics JAZ spectrometer was also used to record the emission response. In this case, a mounted high-power 365 nm LED (M365L2, Thorlabs) was used as an excitation source.

^2H NMR spectroscopy. Variable temperature solid-state ^2H (76.79 MHz) spin echo NMR spectra were collected on a Bruker Avance III-HD 500 MHz spectrometer fitted with a 3.0 mm Doty Scientific static probe. The vendor supplied quadrupole echo sequence was used with a 2.2 μs pulses and 20 μs echo delay. Data was processed after appropriate shifting of the echoes using Bruker Topspin 3.5. Dynamic line-shape fitting was performed with software provided at the NMR Weblab 6.1 (<http://weblab.mpip-mainz.mpg.de/weblab/>).¹⁵

Other physical measurements. FT-IR spectra were obtained on a Perkin-Elmer Spectrum 100. NMR spectra were collected on Bruker Avance III-HD 300 and Bruker Avance III 400 MHz NMR spectrometers. The ^1H and ^{13}C NMR spectra were referenced to natural abundance ^{13}C peaks and residual ^1H peaks of deuterated solvents, respectively. Powder X-ray diffraction patterns were recorded on a Rigaku Miniflex II diffractometer with accelerating voltage and current of 30 kV and 15 mA, respectively. A Waters QTOF-I quadrupole time-of-flight mass-spectrometer was used to record the electrospray ionization mass-spectra.

Table S1. X-ray structure refinement data for *p*COOH-BI-CO₂Me^a and *p*COOH-BI^a.

compound	<i>p</i> COOH-BI-CO ₂ Me	<i>p</i> COOH-BI
formula	C ₁₄ H ₁₂ N ₂ O ₅	C _{26.82} H _{28.56} N ₄ O _{7.95}
FW	288.26	534.12
<i>T</i> , K	100(2)	100(2)
crystal system	triclinic	triclinic
space group	P-1	P-1
<i>Z</i>	4	2
<i>a</i> , Å	9.8035(6)	7.2557(4)
<i>b</i> , Å	11.4779(7)	12.9984(6)
<i>c</i> , Å	12.3921(9)	14.6568(8)
α , °	98.095(2)	106.072(2)
β , °	96.276(2)	97.728(2)
γ , °	108.756(2)	95.999(2)
<i>V</i> , Å ³	1289.30(15)	1301.56(12)
<i>d</i> _{calc} , g/cm ³	1.485	1.363
μ , mm ⁻¹	0.115	0.102
F(000)	600.0	562.0
crystal size, mm ³	0.18 × 0.1 × 0.04	0.46 × 0.24 × 0.14
theta range	4.592 to 50.054	5.02 to 55.512
index ranges	-10 ≤ <i>h</i> ≤ 11 -13 ≤ <i>k</i> ≤ 13 -14 ≤ <i>l</i> ≤ 14	-9 ≤ <i>h</i> ≤ 9 -17 ≤ <i>k</i> ≤ 17 -19 ≤ <i>l</i> ≤ 19
refl. collected	40894	54527
data/restraints/ parameters	4552/2/420	6129/3/388
GOF on F ²	1.041	1.018
Largest peak/ hole, e/Å ³	0.90/-0.39	0.45/-0.29
R ₁ /wR ₂ , [<i>I</i> ≥ 2sigma(<i>I</i>)] ^b	0.0482/0.1126	0.0484/0.1166

^aMo-K α (λ = 0.71073 Å) radiation^b $R_1 = \Sigma ||F_o| - |F_c|| / \Sigma |F_o|$, $wR_2 = \{\Sigma [w(F_o - F_c)^2] / \Sigma [w(F_o)^2]\}^{1/2}$

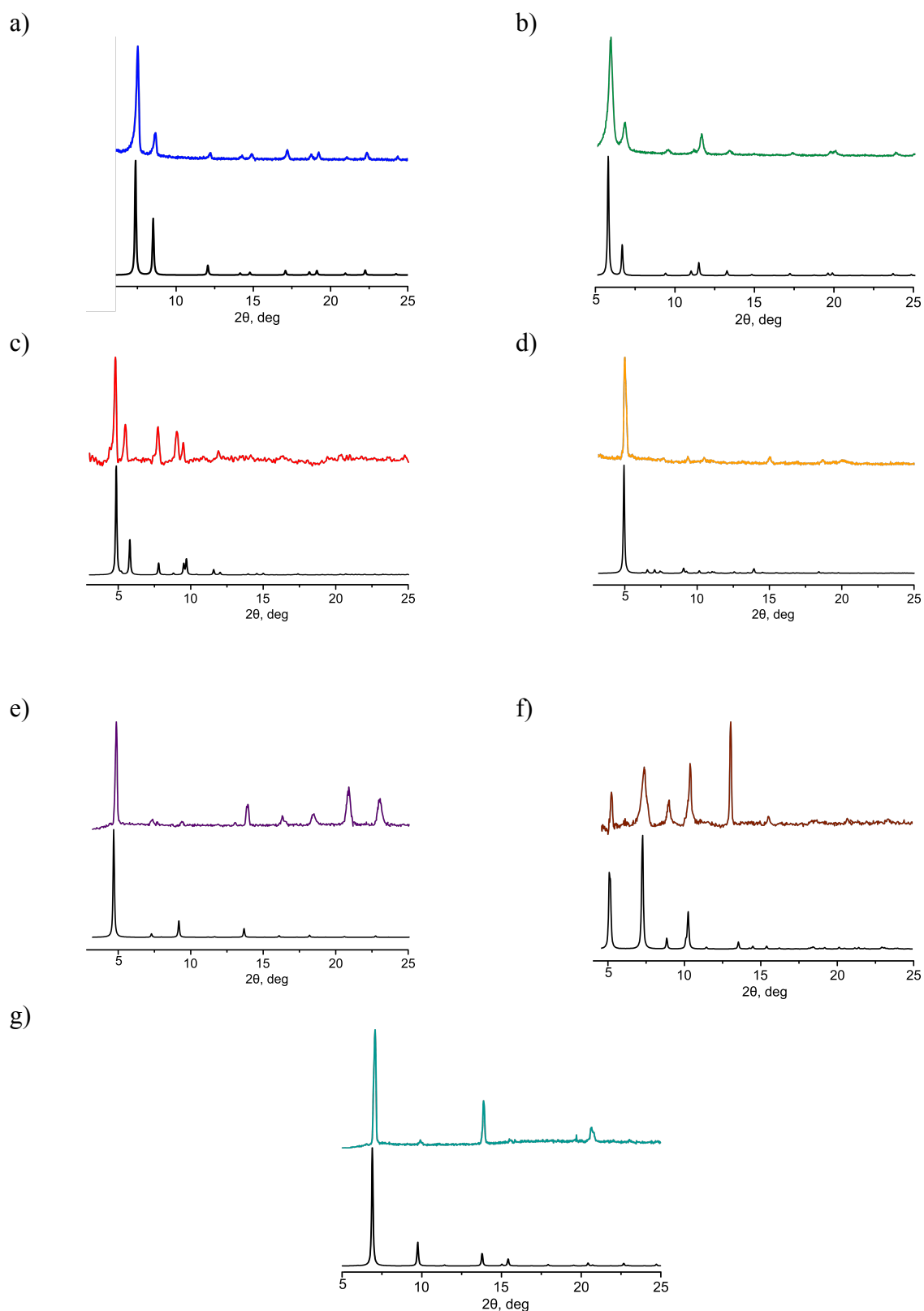


Figure S1. PXRD patterns: a) MeO-*o*HBI@UiO-66, b) MeO-*o*HBI@UiO-67, c) MeO-*o*HBI@UiO-68-NH₂, d) MeO-*o*HBI@Zn₃(BTB)₂, e) MeO-*o*HBI@Zn₆(BTB)₄(BP)₂, f) MeO-*o*HBI@Zr₆O₄(OH)₄(BTB)₂, g) MeO-*o*HBI@MOF-5. For each pair, the top spectrum is experimental, and the bottom spectrum is simulated.

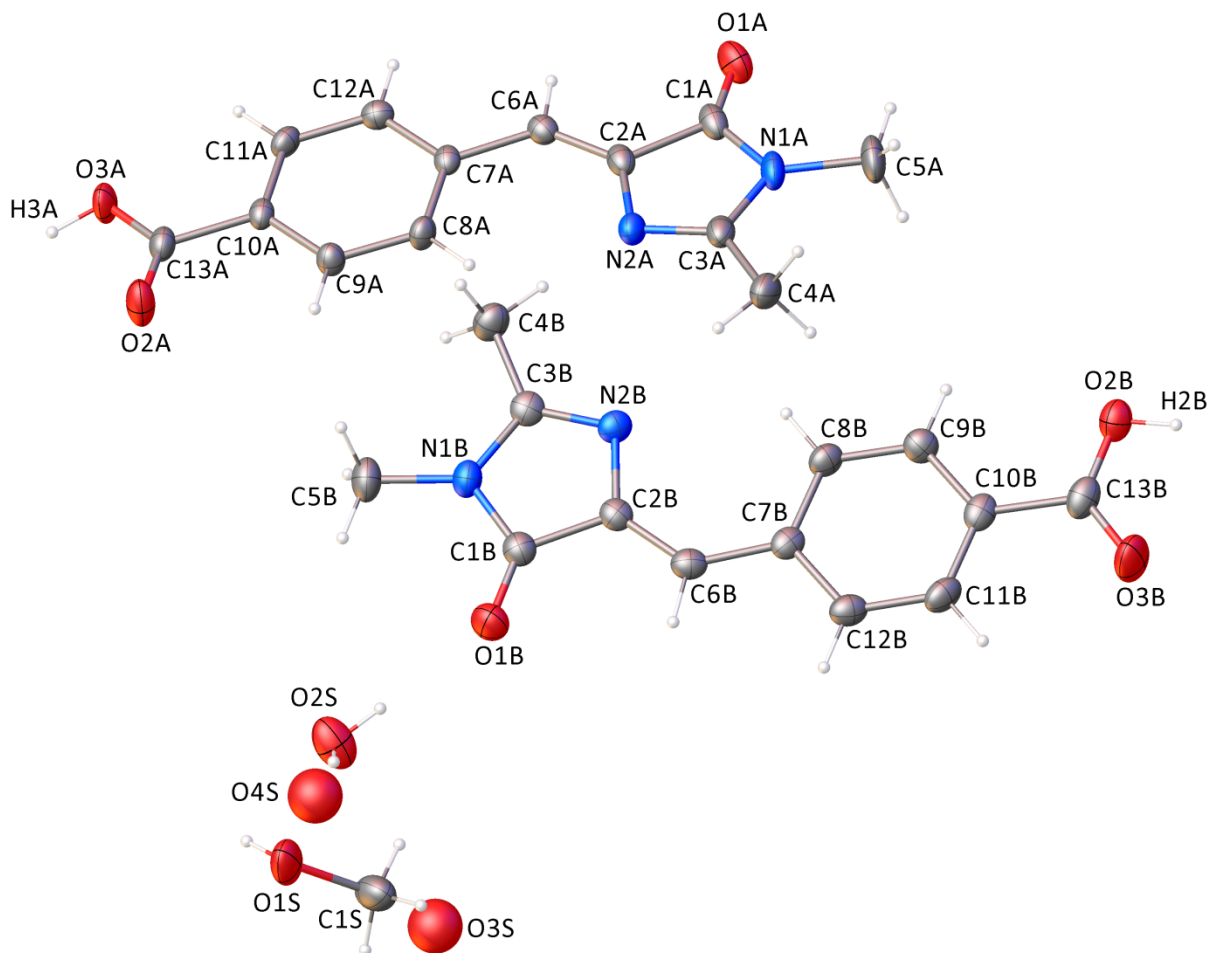


Figure S2. Crystal structure of *p*COOH-BI. Asymmetric unit of the crystal. Displacement ellipsoids drawn at the 60% probability level. Two independent chromophores and a region of solvent modeled as H₂O/H₃O⁺/MeOH. Blue, red, gray, and white spheres represent N, O, C, and H atoms, respectively.

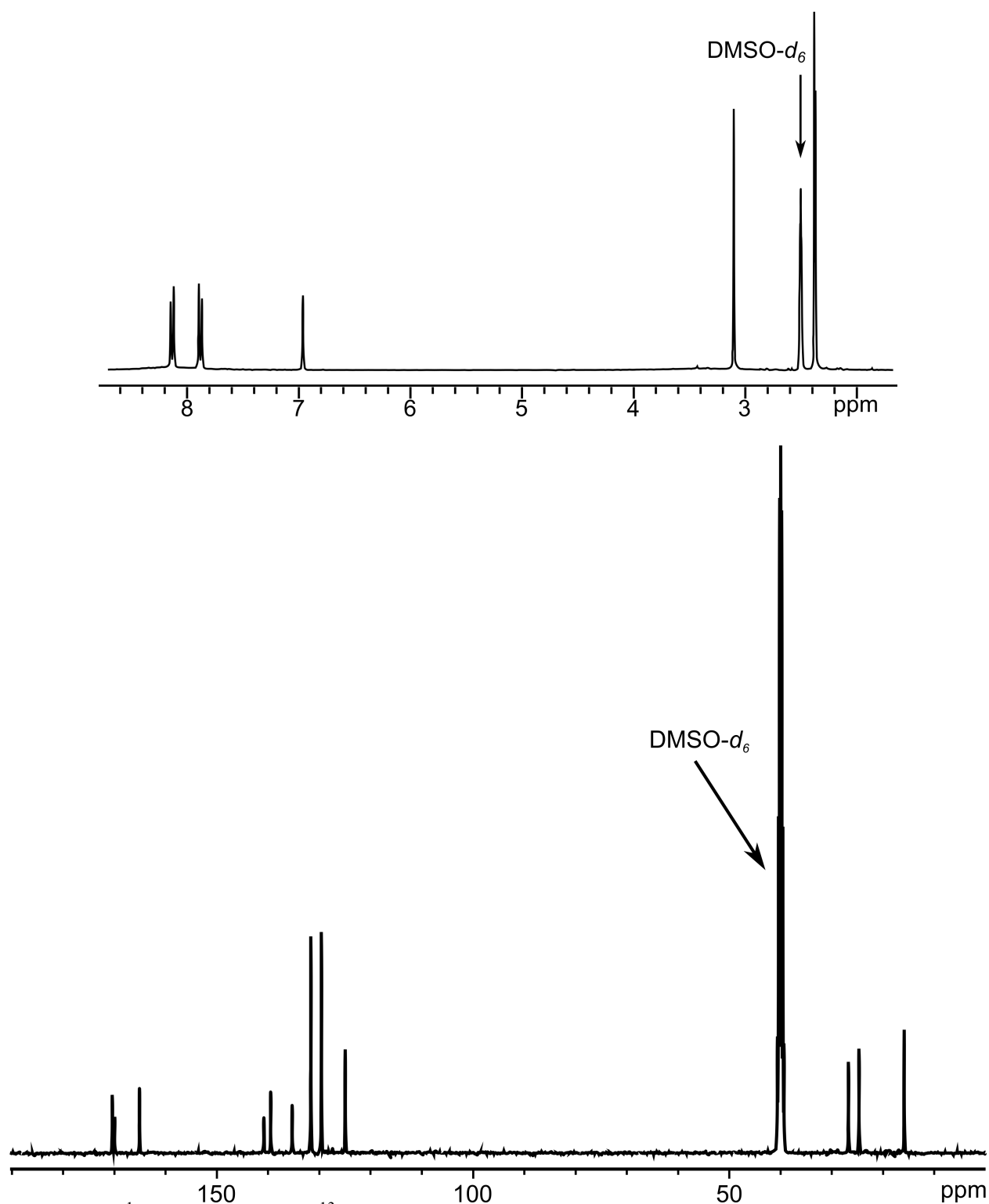


Figure S3. ^1H NMR (*top*) and ^{13}C (*bottom*) spectra of the synthesized *p*COOH-BI chromophore.

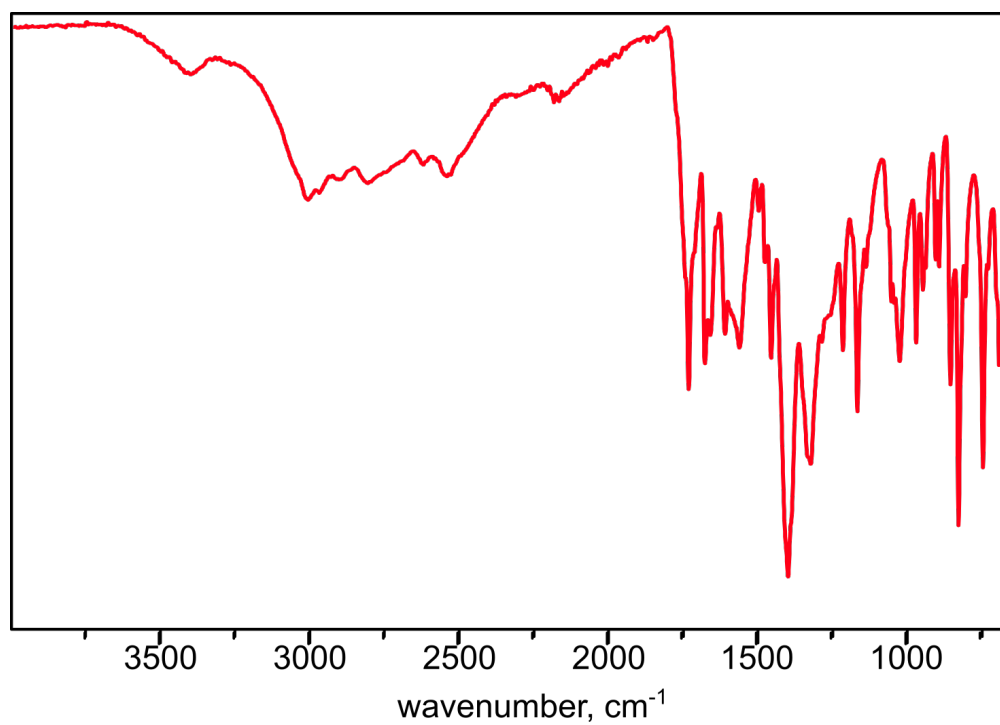


Figure S4. FT-IR spectrum of *p*COOH-BI.

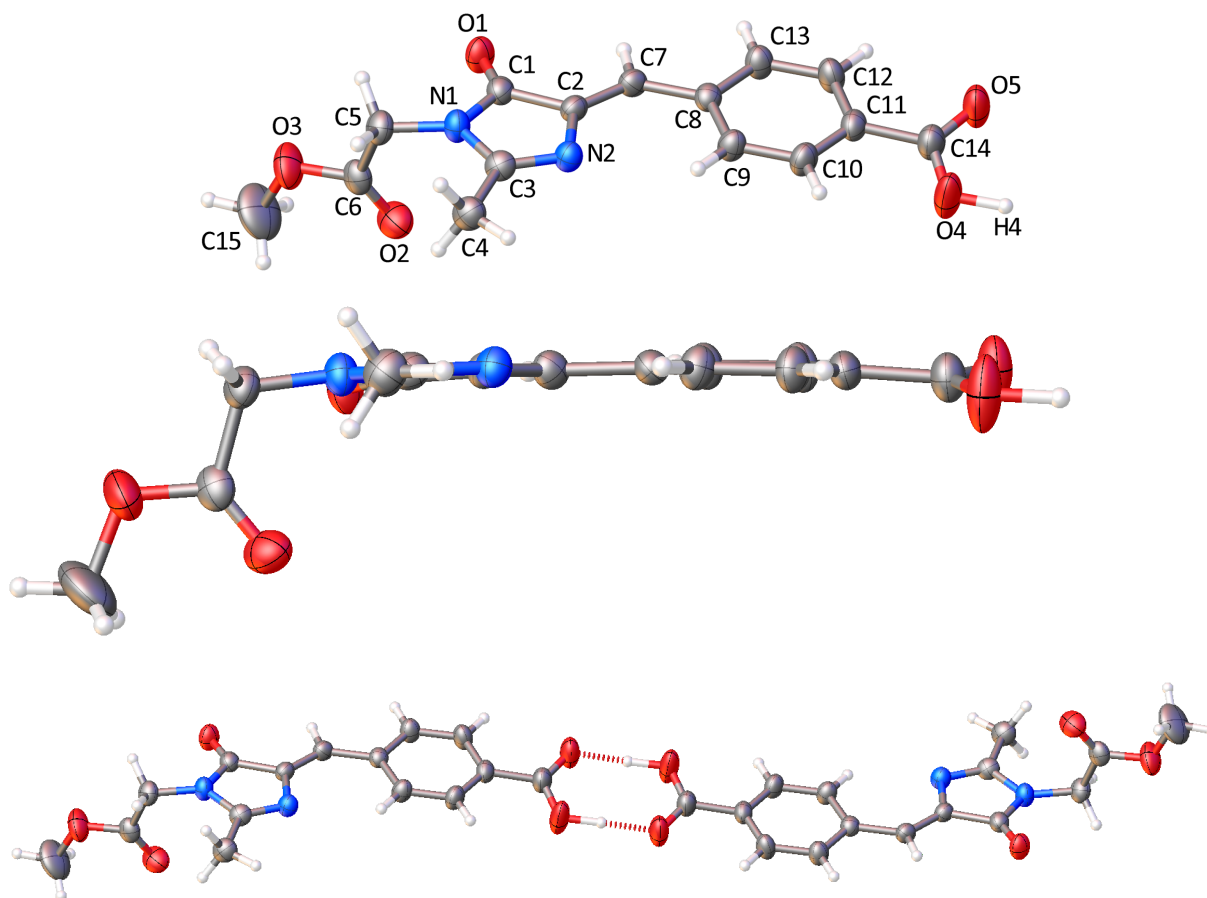


Figure S5. (*top*) Molecular structure of *p*COOH-BI-CO₂Me. (*bottom*) Carboxylic acid dimers. Displacement ellipsoids drawn at the 50% probability level. Blue, red gray and white spheres represent N, O, C and H atoms, respectively.

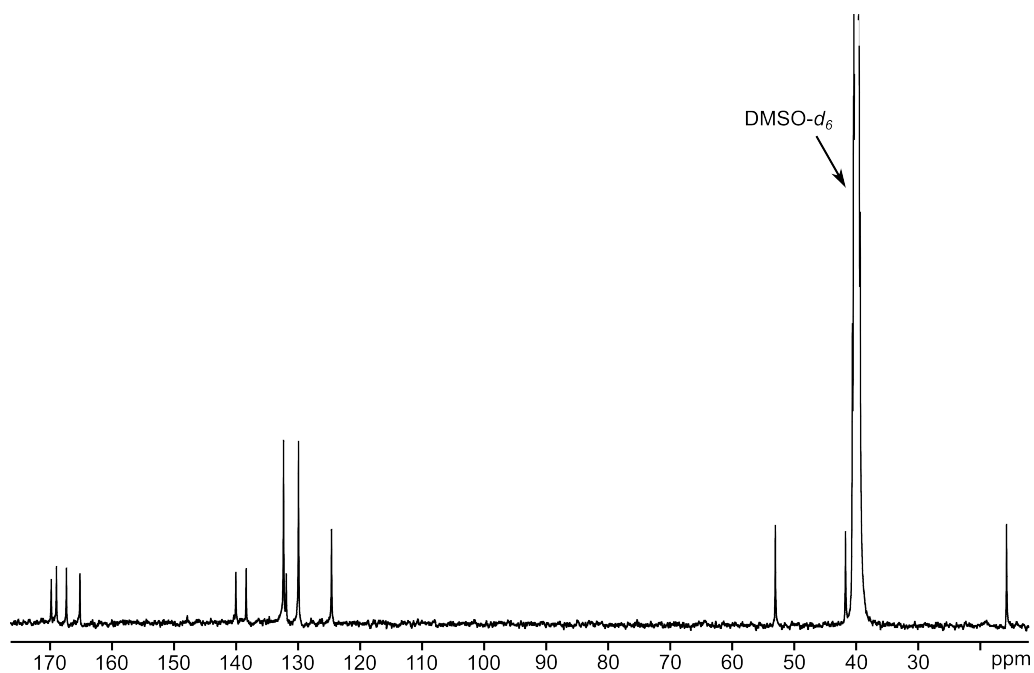
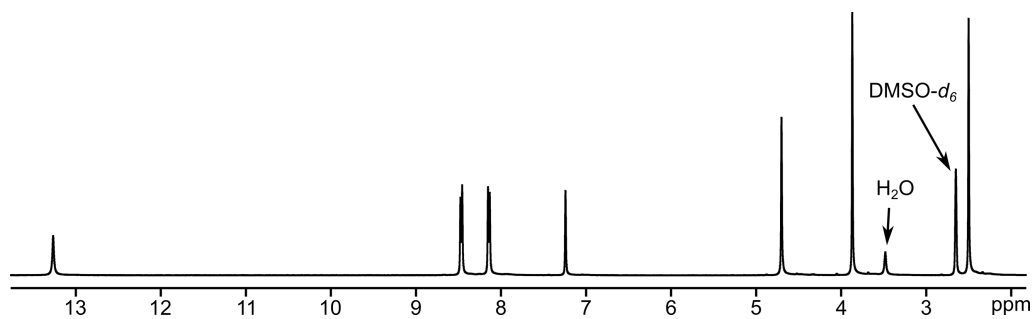


Figure S6. ^1H NMR (*top*) and ^{13}C (*bottom*) spectra of the synthesized $p\text{COOH-BI-CO}_2\text{Me}$ chromophore.

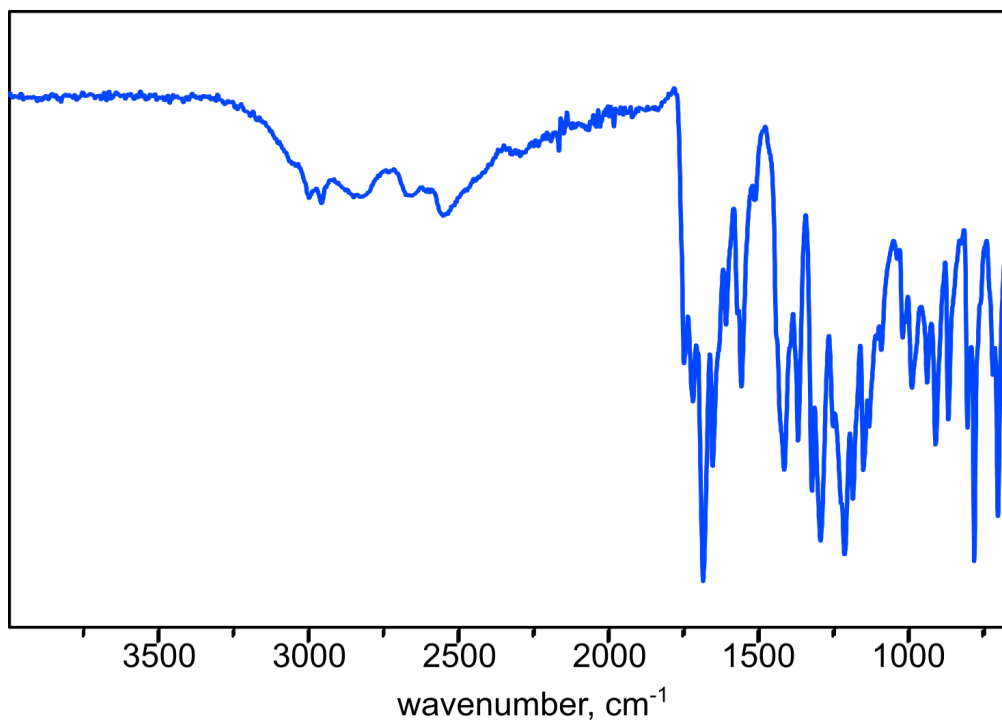


Figure S7. FT-IR spectrum of *p*COOH-BI-CO₂Me.

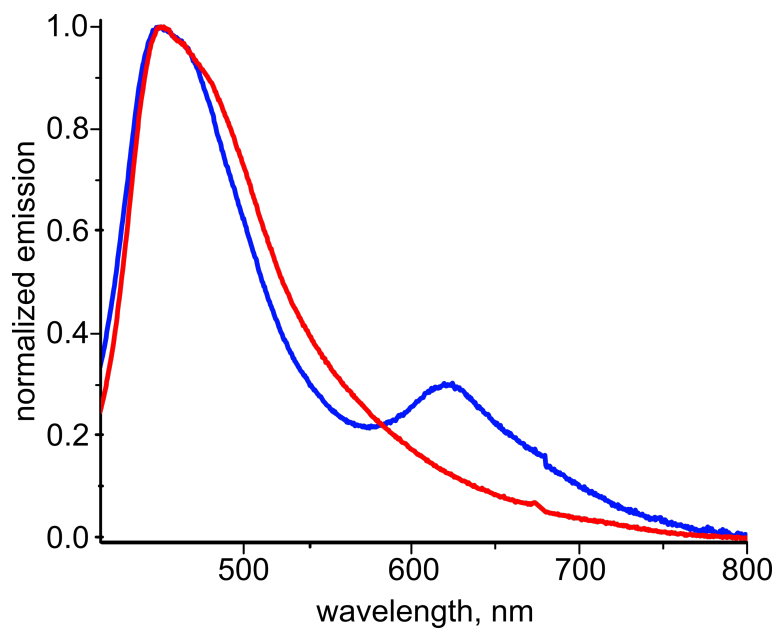


Figure S8. Normalized emission spectra of *p*COOH-BI (red) and *p*COOH-BI-CO₂Me (blue) in the solid state ($\lambda_{\text{ex}} = 350$ nm). The additional peak ~ 620 nm for *p*COOH-BI-CO₂Me most probably corresponds to excimer formation.

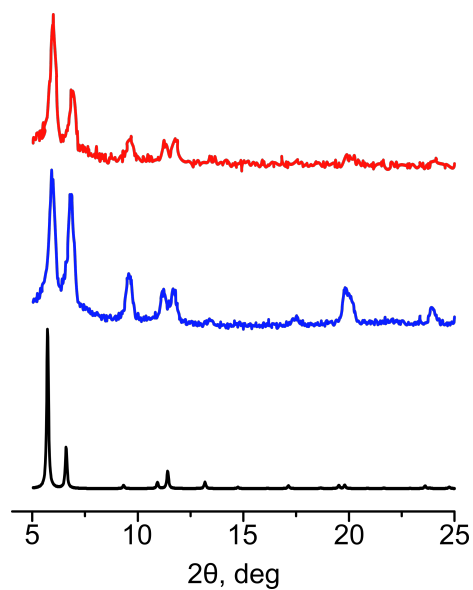


Figure S9. PXR D patterns of $\text{Zr}_6\text{O}_4(\text{OH})_4(\text{BDC-BI-}d_3)_6$: simulated (black), as-synthesized (blue), and after thermal treatment (red).

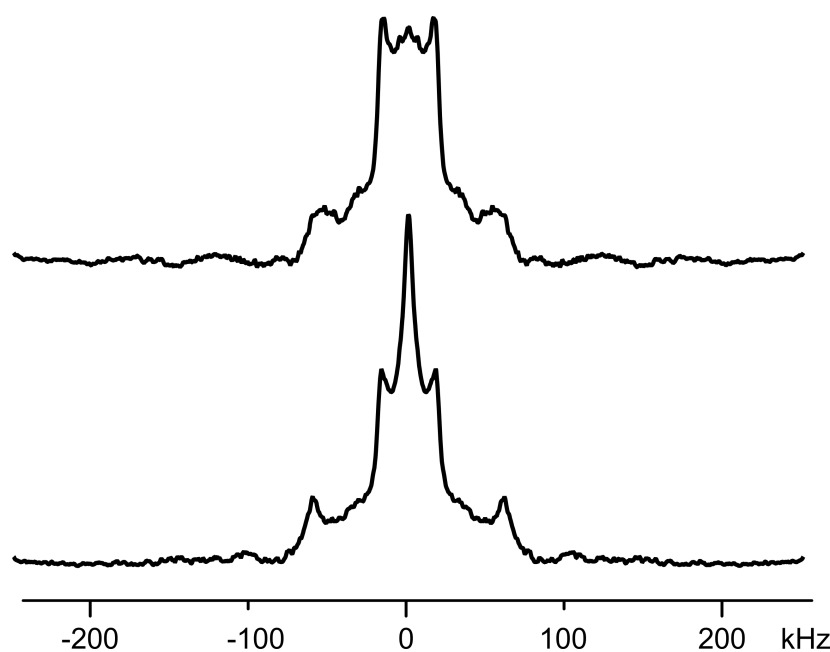


Figure S10. Variable temperature quadrupolar spin-echo solid-state ^2H NMR of $\text{Zr}_6\text{O}_4(\text{OH})_4(\text{BDC-BI-}d_3)_6$ at 50 °C during heating (*bottom*) and cooling (*top*) cycles.

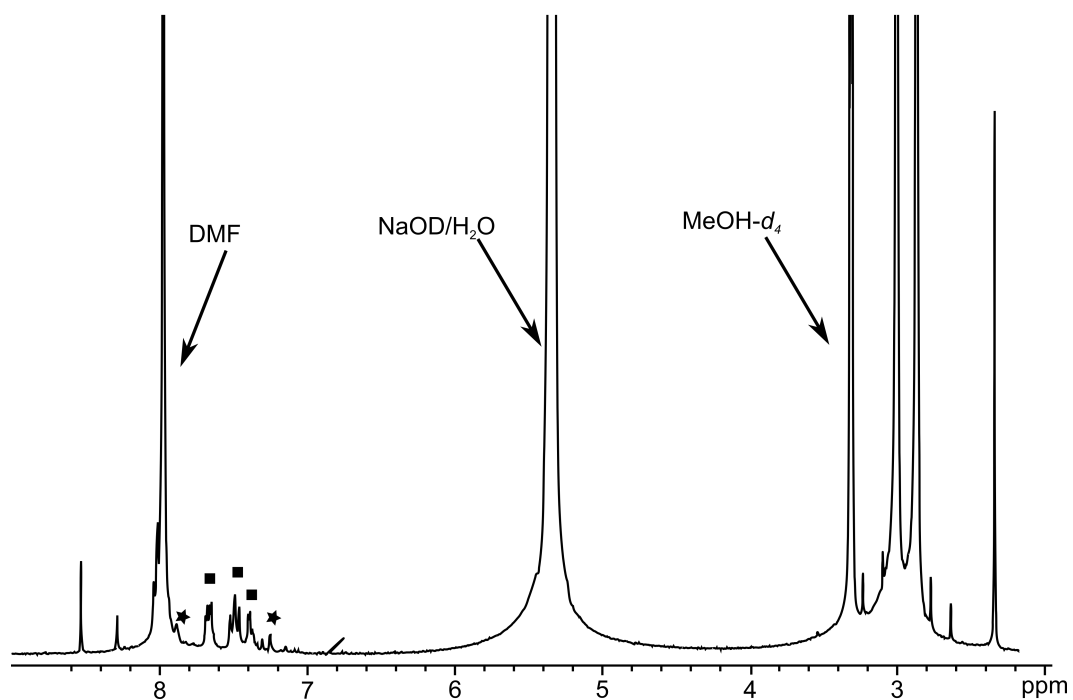


Figure S11. ^1H NMR spectrum of digested UiO-68-NH₂ after “fastened” incorporation of *p*COOH-BI. The peaks corresponding to UiO-68-NH₂ (■) and *p*COOH-BI (*) are labeled.

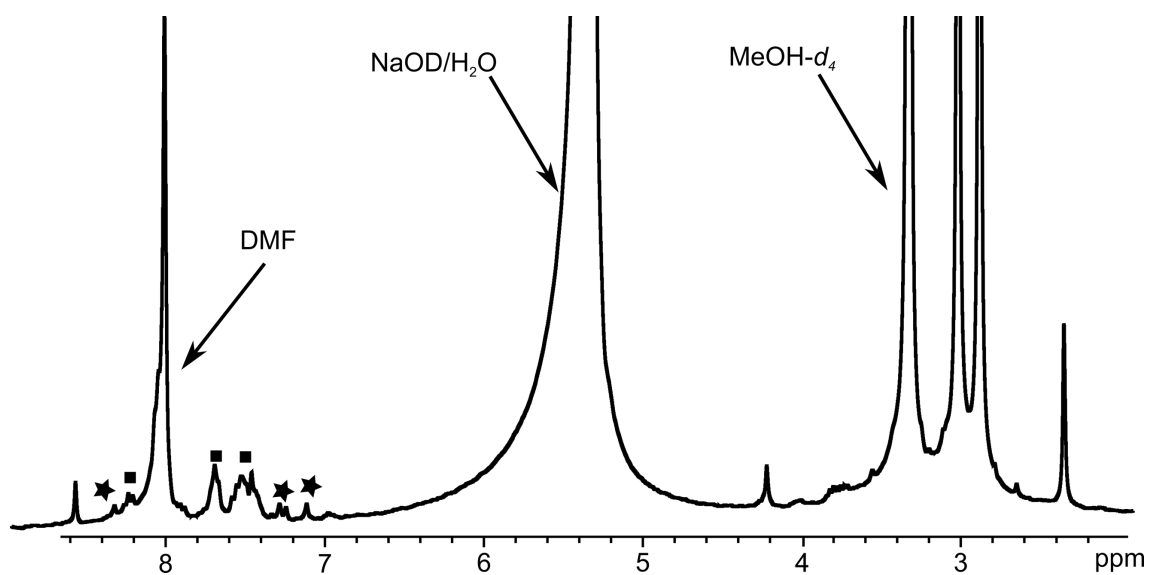


Figure S12. ^1H NMR spectrum of digested UiO-68-NH₂ after “fastened” incorporation of *p*COOH-BI-CO₂Me. The peaks corresponding to UiO-68-NH₂ (■) and *p*COOH-BI-CO₂Me (*) are labeled.

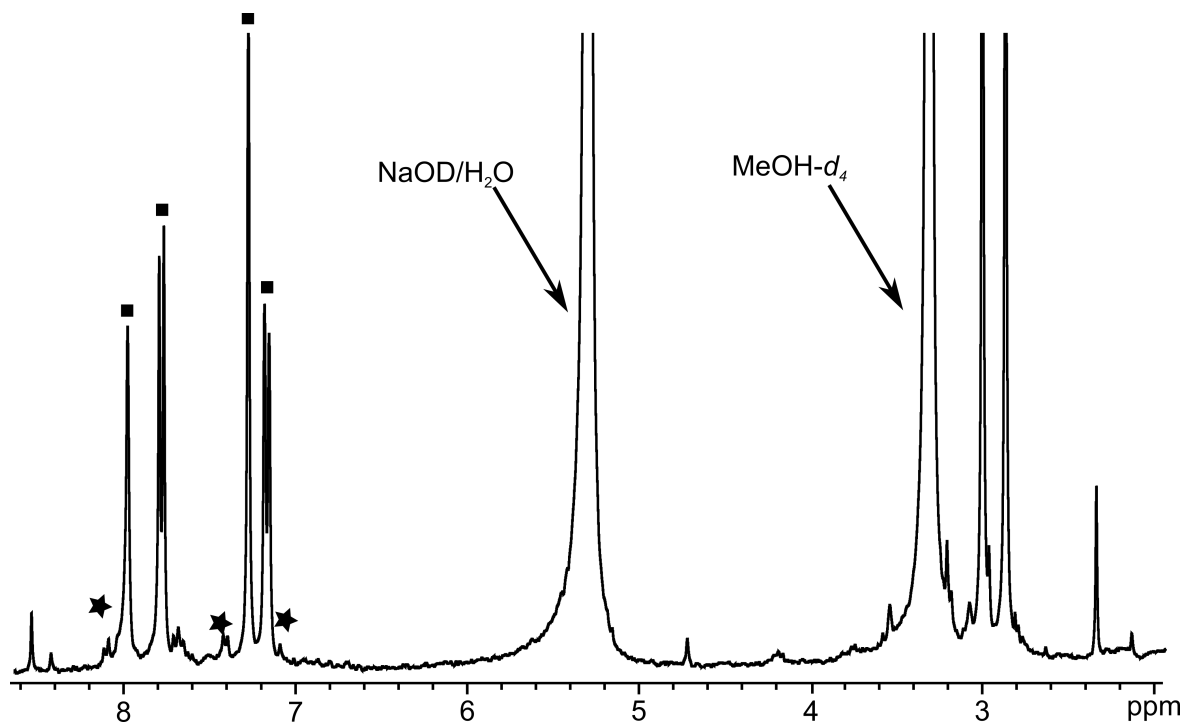


Figure S13. ^1H NMR spectrum of digested MIL-101-Al-NH₂ after “fastened” incorporation of pCOOH-BI. The peaks corresponding to MIL-101-NH₂ (■) and pCOOH-BI (*) are labeled.

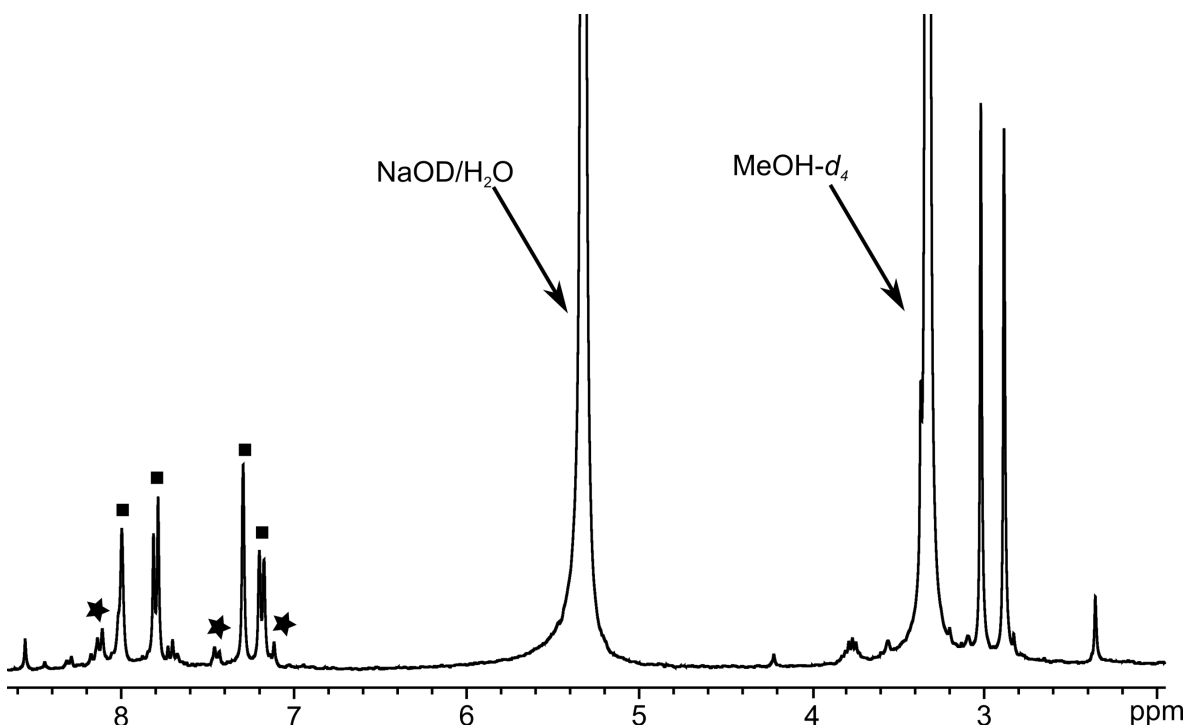


Figure S14. ^1H NMR spectrum of digested MIL-101-Al-NH₂ after “fastened” incorporation of pCOOH-BI-CO₂Me. The peaks corresponding to MIL-101-NH₂ (■) and pCOOH-BI-CO₂Me (*) are labeled.

References:

- 1 J. M. Lerestif, J. Perrocheau, F. Tonnard, J. P. Bazureau and J. Hamelin, *Tetrahedron*, 1995, **51**, 6757.
- 2 E. A. Dolgoplova, T. M. Moore, W. B. Fellows, M. D. Smith and N. B. Shustova, *Dalt. Trans.*, 2016, **45**, 9884.
- 3 H. Hintz and S. Wuttke, *Chem. Commun.*, 2014, **50**, 11472.
- 4 X. Song, S. Jeong, D. Kim and M. S. Lah, *CrystEngComm*, 2012, **14**, 5753.
- 5 K. Schröck, F. Schröder, M. Heyden, R. A. Fischer, M. Havenith, A. J. Skulan, N. R. Moody, B. A. Simmons, M. M. Shindel and M. D. Allendorf, *Phys. Chem. Chem. Phys.*, 2008, **10**, 4732.
- 6 A. Schaate, P. Roy, A. Godt, J. Lippke, F. Waltz, M. Wiebcke and P. Behrens, *Chem. - A Eur. J.*, 2011, **17**, 6643.
- 7 K. Leong, M. E. Foster, B. M. Wong, E. D. Spoerke, D. Van Gough, J. C. Deaton and M. D. Allendorf, *J. Mater. Chem. A*, 2014, **2**, 3389.
- 8 X. Song, T. K. Kim, H. Kim, D. Kim, S. Jeong, H. R. Moon and M. S. Lah, *Chem. Mater.*, 2012, **24**, 3065.
- 9 R. Wang, Z. Wang, Y. Xu, F. Dai, L. Zhang and D. Sun, *Inorg. Chem.*, 2014, **53**, 7086.
- 10 Bruker, *APEX II*, 2013, Bruker AXS Inc., Madison, Wisconsin, USA.
- 11 G. M. Sheldrick, *Acta Cryst.*, 2008, **A64**, 112.
- 12 G. M. Sheldrick, *Acta Cryst. C*, 2015, **71**, 3.
- 13 O. V. Dolomanov, L. J. Bourhis, R. J. Gildea, J. A. K. Howard and H. Puschmann, *J. Appl. Crystallogr.*, 2009, **42**, 339.
- 14 L. Krause, R. Herbst-Irmer, G. M. Sheldrick and D. Stalke, *J. Appl. Crystallogr.*, 2015, **48**, 3.
- 15 V. Macho, L. Brombacher and H. W. Spiess, *Appl. Magn. Reson.*, 2001, **20**, 405.